Implementation of Brushed DC Motor Control in LabVIEW FPGA

Krisztián Lamár
Institute of Automation
Óbuda University
Budapest, Hungary
lamar.krisztian@kvk.uni-obuda.hu

András Gergő Kocsis
Department of Electrical Machines and Drives
Budapest University of Technology and Economics
Budapest, Hungary
kocsis_gergo@chello.hu

Abstract— **The paper introduces the fundamentals of motor control. It explains the basic equations and introduces the control diagram of the brushed DC motor. It introduces the four quadrant DC chopper circuit and the basic methods to operate it. After that, it explains the fundamentals of the current control of DC motors and its two basic methods: the pulse width modulation and the hysteresis current control. Finally it gives a short example of the practical implementation of the hysteresis current controller for the four quadrant DC chopper in LabVIEW FPGA.**

Keywords— *permanent magnet brushed DC motor, four quadrant DC chopper, pulse width modulation, current control, LabVIEW FPGA*

I. INTRODUCTION

The purpose of motor controls is to control the torque, speed and position of a motor. Since the torque of the motor is proportional to its current, direct torque control is very rarely used. In almost every application cascade control structure is used as show in Fig. 1 [4].

This means that the drive electronics that supplies the motor gets its control signals from the current controller, which gets its set point from the speed controller and so on. The current controller is called drive specific, since its operation is greatly affected by the type of the motor. The position and speed controller is called task specific because it is more affected by the machine being driven by the motor [4].

II. MOTOR CONTROL FUNDAMENTALS

It is not necessary to use all three of these controls in every application. In some cases position or speed control is not needed but current control is used in every case. The reason of this is that the current control not only ensures stable and controlled torque but gives the possibility to limit the current of the machine, and with this function, it is able to protect it from overload [3]. The three controllers run at different speeds. For example the current controller is way faster than the speed controller.

The feedback values of the controllers have to be measured. Measuring the current can be done with a shunt resistor or Hall Effect current transducers. For speed and position measurement quadrature encoders can be used [7][10]. For position control usually proportional (P) or rarely proportional-differential (PD) controllers are used. The type of the speed controller is usually proportional-integral (PI). The current control can be realized with proportional-integral (PI) or hysteresis controller [8].

III. BRUSHED DC MOTORS

Unlike its construction, the control of brushed DC motors is simple compared to the other motor types [8]. The most frequently used DC machine types are the permanent magnet and the separately excited ones [4]. In this article, the current control of a permanent magnet DC motor is explained. The equivalent circuit of these motors is shown in Fig2.
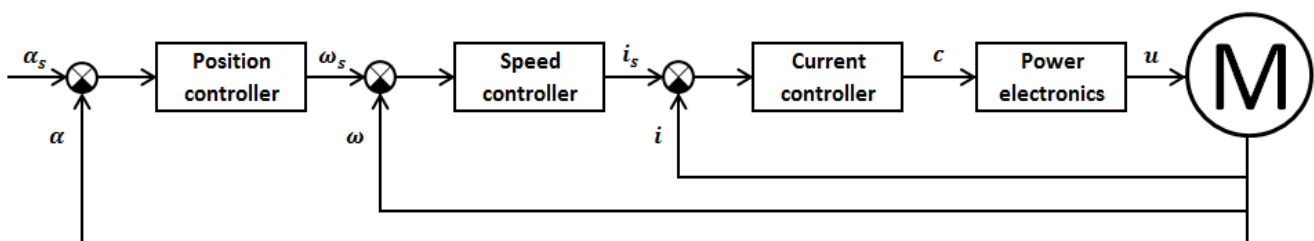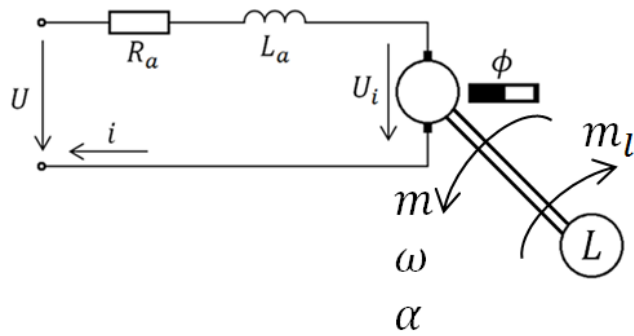

Fig. 1. The cascade control structure

Fig. 2. The equivalent circuit of a permanent magnet brushed DC motor

The meanings of the symbols in Fig. 2 are the following: R_a is the armature resistance, L_a is the inductance of the armature. U is the voltage, and i is the current of the motor, while U_i is the induced voltage. ϕ is the flux, ω is the angular velocity, α is the angle and m is the torque of the motor. L is the load connected to the shaft of the motor, and m_l is the torque of the load.

The following equations apply to this circuit [3]:

$$U = i \cdot R_a + L \cdot \frac{di}{dt} + U_i \qquad (3.1)$$

$$U_i = k \cdot \phi \cdot \omega \qquad (3.2)$$

$$m - m_l = \Theta \cdot \frac{d\omega}{dt} \qquad (3.3)$$

$$m = k \cdot \phi \cdot i \qquad (3.4)$$

$$\omega = \frac{d\alpha}{dt} \qquad (3.5)$$

The symbols used in these equations are the same that was used in Fig. 2. The exceptions are the k, which is a constant and the Θ which is the inertia of the load and the machine. By transforming the equations (3.1…3.4) to the Laplace space, the control diagram, (shown in Fig3) can be drawn [4]. The symbol T_e on the diagram is the electric time constant, the definition of this constant is $T_e = \frac{L_a}{R_a}$. It can be seen on the diagram, that current can only be altered effectively by the voltage connected to the motor. By altering the voltage, the current can be even controlled, if it is being measured.
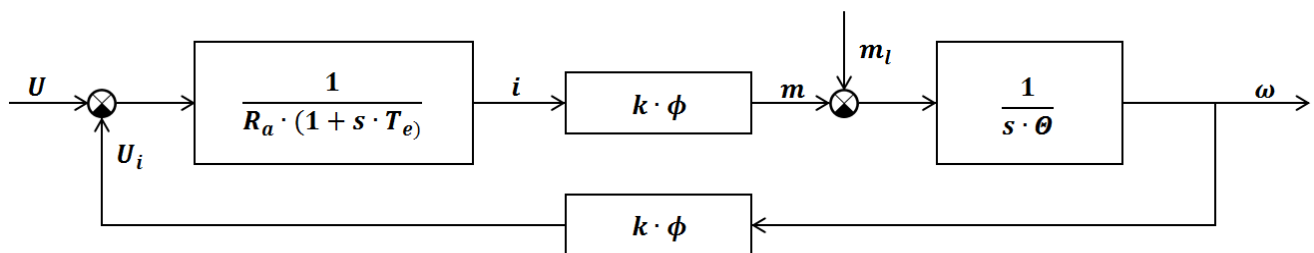
IV.   THE FOUR QUADRAND DC CHOPPER

With the four quadrant DC chopper circuit (shown on Fig 4.), the controlled supply of a brushed DC motor is possible. The circuit consist four transistors ($T1…T4$). Each transistor has a freewheeling diode to conduct the current of the motor, when the transistor is switched off [3].
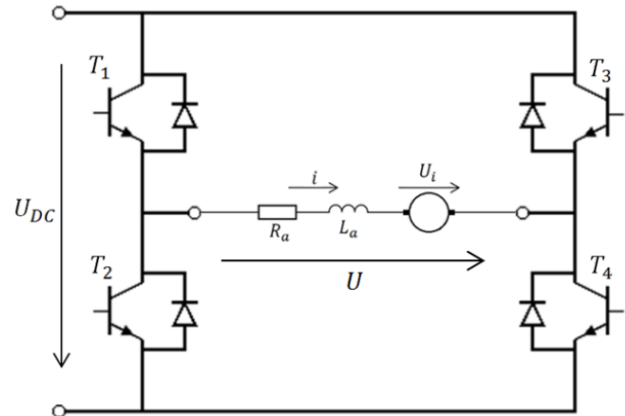

Fig.4. The four quadrant DC chopper with a brushed DC machine

The circuit needs a DC voltage supply shown in Fig3 with symbol U_{DC}. The circuit is called four quadrant because it can drive and brake the motor is both directions. When the transistors T_1 and T_4 are switched on, the circuits supplies the motor with positive voltage, shown in Fig. 4 with symbol U. Switching on the transistors T_2 and T_3, the motor is supplied with negative voltage. Switching on the transistors T_1 and T_2 or T_3 and T_4 simultaneously have to be avoided, because this leads to a short circuit between the two terminals of the circuits input. Because of this, a certain amount of time has to be elapsed between switching positive and negative voltages to the motor. This time is called the dead time [8].The length of the dead time depends on the switching times of the transistors used in the circuit.

With switching the transistors on and off in a controlled way, a so called pulse width modulation (PWM) supply of the motor can be realized [6]. The fundamentals of the PWM supply can be seen in Fig. 5. Every period (T) consists of two parts: the on time (t_{on}) while the transistors T_1 and T_4 are switched on, providing a positive U_{DC} voltage for the motor, and the off time (t_{off}), while the circuit connects zero voltage to the motor. The length of every period is the same, and it is

Fig. 3. The control diagram of a permanent magnet brushed DC machine

calculated from the switching frequency [5]. With increased switching frequency, smoother current (and torque) can be achieved, but the switching losses will be higher.
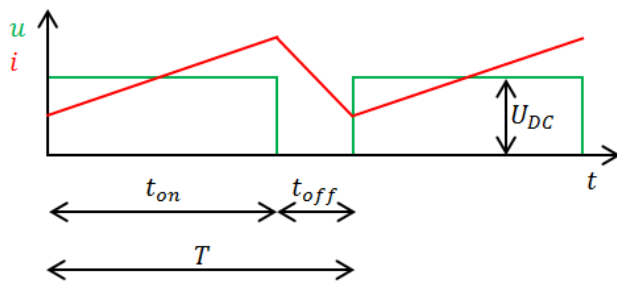

Fig. 5. The pulse width modulation supply

The two basic types of the PWM are the unipolar and the bipolar. When using the unipolar PWM, positive or negative voltage is connected to the motor during the on time, and in the off time, zero voltage is supplied to the motor, as shown in Fig. 5. When the bipolar PWM is used, opposite polarity voltage is connected to the motor during the off time [3].

The ratio off the on time and the length of the period is called the duty cycle (D) [4]:

$$D = \frac{t_{on}}{T} \cdot 100\% \qquad (4.1)$$

The average voltage of the motor during a period can be calculated with the duty cycle. The equations for the unipolar and the bipolar PWM are different [8]:

$$U_{uavg} = \frac{t_{on} \cdot U_{DC} + t_{off} \cdot 0}{T} = D \cdot U_{DC} \qquad (4.2)$$

$$U_{bavg} = \frac{t_{on} \cdot U_{DC} - t_{off} \cdot U_{DC}}{T} = \frac{t_{on} \cdot U_{DC} - (T - t_{on}) \cdot U_{DC}}{T} =$$

$$= (2 \cdot D - 1) \cdot U_{DC} \qquad (4.3)$$

Zero voltage can be produced with the circuit by switching all four transistors off, or by switching T_1 and T_3 or T_2 and T_4 on. The advantage of the last two methods is that the discontinuous conduction can be avoided [8].

V.   CURRENT CONTROL

As it was mentioned before, by controlling the current of the motor, its torque can be controlled. The current controller gets its set point from the speed controller, and by subtracting the measured current value from it, the current error, i_e can be calculated. From the error, the input parameters of the DC chopper can be calculated. There are two basic methods for controlling the current: the pulse width modulation and the hysteresis current control. These two methods differ in the number of required calculations and in their switching frequency.
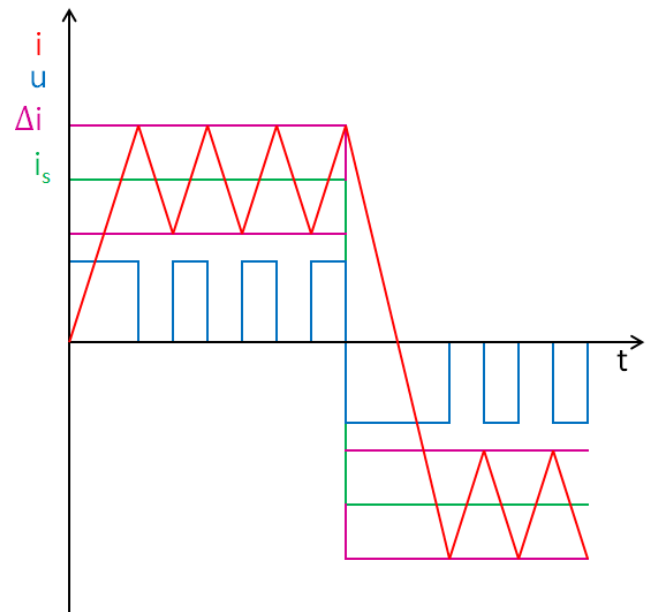

Fig. 6. The operation of the hysteresis current controller

A.   The hysteresis current controller

This method is constantly comparing the actual value of the motor current with the set point. If the difference is larger than the hysteresis, then the controller changes the control signals of the DC chopper, so the current will head toward the set point [3]. The operation of the hysteresis current controller can be seen in Fig. 6, where i_s is the current set point and Δi is the hysteresis window. The size of the hysteresis window can be set in the motor control program. The lower this value is, the smoother is the current of the motor, but the switching frequency will increase. The smoothness of the current is limited by the maximum frequency of the current measurement and the DC chopper circuit. With this method, the measurement of the motor current has to be done as often as it is possible.

The hysteresis current controller can work in unipolar (shown in Fig. 6) and bipolar modes [3]. The advantage of this method is that it only requires a few simple calculations, and it does not require any parameter setting beside the width of the hysteresis window. Because of this, this controller is often called robust.

B.   Pulse width modulation current controller

This method calculates the duty cycle (4.1) of the pulse width modulation from the current error using a PI controller [6]. From the duty cycle, the parameters of the pulse width modulation can be calculated. The equations of the PI controller can vary based on the type of the integration method being used. The equations with the midpoint integration [9]:

$$i_e(k) = i_s(k) - i(k) \qquad (5.1)$$

$$y_{PI}(k) = K_p \cdot i_e(k) + \frac{K_p \cdot T_s}{T_i} \cdot \sum_{i=1}^{k} \left[\frac{i_e(i) + i_e(i-1)}{2}\right] \quad (5.2)$$

_____

Where y_{PI} is the output signal, K_p is the gain, T_s is the sampling time, and T_i is the integral time of the PI controller, i_e is the current error. The PI controller usually has an adjustable output limit, and a so called anti-windup function, which stops the integrator when the output reached the limit. After the PI controller calculated the duty cycle, the actual switching points (shown in Fig. 5) can be easily defined.

Unlike the hysteresis current control, the measurement of the motor current has to be synchronized to the PWM cycle. This means that this method has a well-defined current measurement point in every period. The measurement of the motor current has to be done when the current is at its average level during the period. There are two points suitable for the measurement in every cycle: the middle of the on and the middle of the off time. The measurement is easier in the longer part of the period [7].

The pulse width modulation current control can also work in both unipolar and bipolar modes. The advantage of this method is that it required lower switching frequencies and the motor current do not have to be measured as often. The disadvantage is that, the PI controller has to be tuned, and this method needs a lot more calculation than the hysteresis current control.

VI. IMPLEMENTATION OF THE HYSTERESIS CURRENT CONTROL IN LABVIEW FPGA

The following example describes the algorithm and the implementation of the hysteresis current controller in LabVIEW FPGA. The program has two loops that run parallel. One of them is the current controller, and the other is controlling the operation of the DC chopper. The current controller loop – shown in Fig. 7 - is responsible for measuring the current of the motor with a well-defined frequency (0,1 MHz is used in this example), and comparing the result with the value of the current set point with an adjustable hysteresis window.
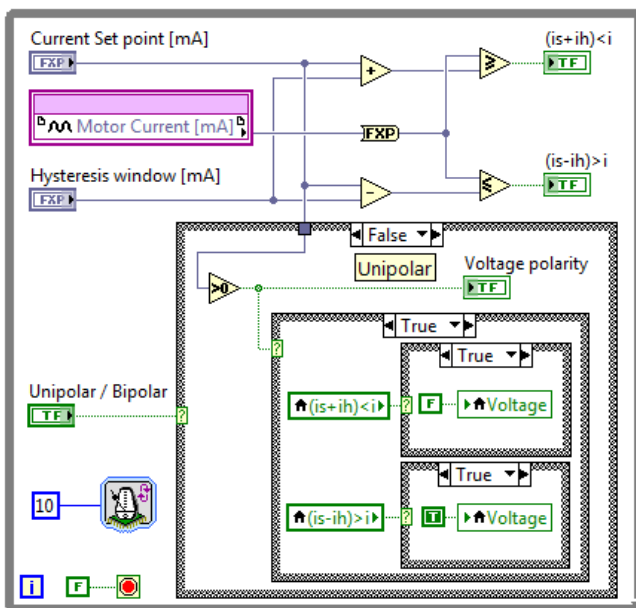

Fig. 7. The loop of the hysteresis current controller with the unipolar case

In this example, it is assumed that the measurement gives the result in milliamps, and there is no need for scaling, offset and linearity error compensation. The result of the comparison is stored in two Boolean variables. If the value of the "$(is + ih) < i$" variable is true then the current of the motor is higher than the current set point plus the hysteresis window. If the "$(is - ih) > i$" variable is true then the actual current is lower than the set point. From these variables, the necessary action of the DC chopper can be determined.

The controller has an input variable for selecting between the unipolar and bipolar modes. In Fig. 7, the unipolar case is shown. The controller gives orders to the DC chopper trough two variables: the "Voltage" and the "Voltage polarity" bits. In the unipolar mode, the polarity is simply determined by the sign of the current set point. Depending on the polarity, the "Voltage" variable is controlled by the "$(is + ih) < i$" and the "$(is - ih) > i$" bits. For example if the current set point is positive then positive voltage have to switched by the DC chopper if the "$(is - ih) > i$" is true.

When the actual current enters the hysteresis window, then the two comparison variables will change to false. The last state of the DC chopper remains active until the current reaches the other side of the hysteresis window. To ensure this, the false cases of the two case structure controlled by the comparison variables are empty.

The case of the bipolar mode – shown in Fig. 8 – is a bit simpler than the unipolar case. The "Voltage" variable is always switched on because of the nature of the bipolar mode. This mode only operates with the "Voltage polarity" variable. The inner case structures works similarly to the unipolar mode: if the current is higher than the hysteresis window then negative, if it is lower, then positive voltage polarity order is sent to the loop of the DC chopper. The false cases of the inner case structures are empty in this mode either.
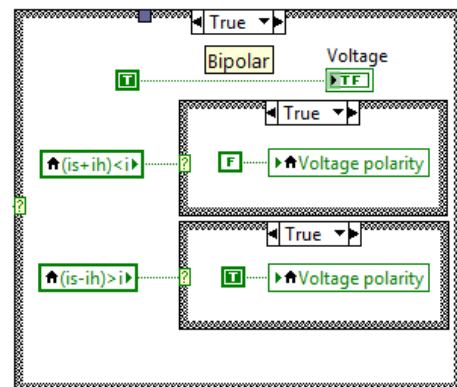

Fig. 8. The bipolar case of the hysteresis current controller

The purpose of the DC chopper loop – shown in Fig.9 - is to ensure that the circuit is switching the necessary voltage - what has been selected by the current controller loop - to the motor, and to ensure that the necessary dead time is inserted between the switches. The loop is realized with a single cycle timed loop with ten megahertz clock frequency. This means that the content of the loop is executed in every 100 nanosecond [1].
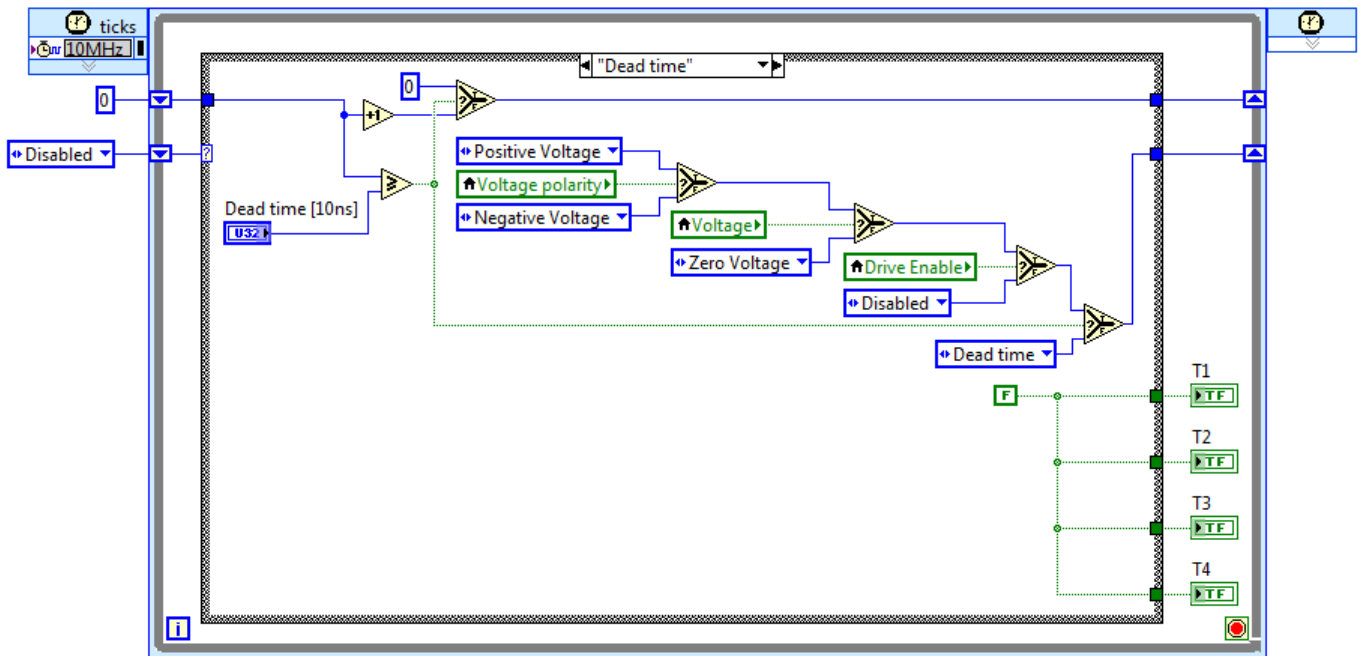
Fig. 9. The DC Chopper loop with the Dead time case

The loop has four input variables: the "Voltage" and "Voltage polarity" variables, and the "Drive Enable" and "Dead time [10ns]" variables. The output variables are the signals of the four transistor (T1..T4). Inside the loop there is a state machine, realized by a case structure [2], with the following states: dead time, disabled, zero voltage, positive voltage, negative voltage.

The dead time state (shown in Fig. 9) is basically a simple timer. After the adjustable dead time elapsed, the state machine switches to the next state, what is determined by the input variables trough three select functions [2]. While the program is in this state, the four transistors are switched off.

The disabled state is going active if the "Drive Enable" variable changes to false. The transistors are switched off in this state either. After enabling the drive, the state machine goes to one of the voltage states.

The zero, positive and negative voltage cases are similar to each other. The transistors signals are the following in these cases: T_1 and T_4 are switched in the positive case, T_2 and T_3 are switched in the negative case and in the zero voltage case T_2 and T_4 transistors are switched on to prevent the discontinuous conduction. The exit conditions are defined by the input variables.

VII. Conclusion

The current control is a basic function of modern electric drives. The reason of this is that it not only ensures a controlled torque but it gives a protection from overload [3]. As it can be seen in this paper, the theory of current control with the four quadrant DC chopper is simple. The two basic methods, the pulse width modulation and the hysteresis current controls are differ in the number and complexity of the necessary calculations and in the required frequency of current

measurement and switching. If the used hardware enables the frequent current measurement and switching then the hysteresis current controller can be a good solution, since it has a robust operation and it does not require tuning and too much calculation.

REFERENCES

[1] National Instruments, "LabVIEW FPGA module user manual" Mar, 2004

[2] National Instruments, "LabVIEW user manual" Apr, 2003

[3] I. Schmidt, Gy-né. Vincze, K. Veszprémi, "Villamos szervo- és robothajtások", Műegyetemi Kiadó, 2000.

[4] I. Schmidt, K. Veszprémi, "Drive Control", https://vet.bme.hu/sites/default/files/tamop/vivem175en/out/html/vivem 175en.html (accessed 30-09-2013)

[5] Baldor Electric Company, "Servo Control Facts", http://www.baldor.com/pdf/manuals/1205-394.pdf (accessed 30-09-2013)

[6] F.H. Ali, M.M. Hussein, S.M.B. Ismael, "LabVIEW FPGA Implementation Of a PID Controller For D.C. Motor Speed Control", Irac J. Electrical and Electronic Engineering, Vol. 6 No.2, 2010

[7] K. Veszprémi, "Mikroszámítógépes hajtásirányítás", Budapesti Műszaki és Gazdaságtudományi Egyetem, 2012

[8] L. Számel, "Szervo és robothajtások", Budapesti Műszaki és Gazdaságtudományi Egyetem, 2013

[9] National Instruments, "LabVIEW: PID and Fuzzy Logic Toolkit User Manual", June 2009

[10] Lamár, K., Kocsis, A.G., Implementation of Speed Measurement for Electrical Drives Equipped with Quadrature Encoder in LabVIEW FPGA, Acta Technica Corviniensis – Bulletin Of Engineering, Vol.6. No.4. pp.123-126. 2013.

[11] Kiraly, I., Determination of correction coefficients of the slot leakage inductance for multi-phase machines, COMPEL-The International Journal for Computation and Mathematics in Electrical and Electronic Engineering, Vol.32, No.3, pp. 961-976, 2013

_____

[12] Varga, A., Rácz, E., Kádár, P., New Experimental Method for Measuring Power Characteristics of Photovoltaic Cells at Given Light Irradiation, Proceedings of 8th IEEE International Symposium on Applied Computational Intelligence and Informatics, SACI-2013, Timisoara, Romania, pp.405-409, 2013

[13] Fuerstner, I., Gogolak, L., Pletl, S., Solution Diversity for a Specified Project in Mechatronics, Proceedings of the International Conference Science in Parctice, 2012

[14] Novak-Marcincin, J., Janak, M., Barna, J., Torok, J., Novakova-Marcincinova, L., Fecova, V., Verification of a program for the control of a robotic workcell with the use of AR, International Journal of Advanced Robotic Systems, Vol.9, Art. No. 54, 2012

[15] Rădac, M.-B., Precup R.-E., Petriu, E. M., Preitl, S., Experiment-based Performance Improvement of State Feedback Control Systems for Single Input Processes, Acta Polytechnica Hungarica, Vol.10, No.3, pp.5-24, 2013

[16] Sárosi, J., Accurate Positioning of Humanoid Upper Arm, International Journal of Engineering, Annals of Faculty of Engineering Hunedoara, Vol. 9, No. Extra, pp. 33-36, 2011

[17] Durovsky, F., Fedak, V., Integrated mechatronic systems laboratory, Proceedings of the 14th International Power Electronics and Motion Control Conference (EPE-PEMC 2010), pp.S51-S55, 2010

[18] Suto, J., Oniga, S., Remote controlled data collector robot, Carpathian Journal of Electronic and Computer Engineering., Vol.5. pp.117-120, 2012

[19] Györök, Gy., Makó, M., Lakner, J., Sensorless D.C. Motor Control with Predictive Sensig Methode, ÓBUDA UNIVERSITY E-BULLETIN Vol.1, No.1, pp.51-59, 2010

[20] Györök, Gy., Sensorless DC Motor Control, Proceedings of 11th International Carpathian Control Conference ICCC-2010, pp.71-74, 2010

[21] Szénási, S., Vámossy, Z., Implementation of a Distributed Genetic Algorithm for Parameter Optimization in a Cell Nuclei Detection Project, Acta Polytechnica Hungarica, Vol.10, No.4, pp 59-86, 2013

[22] Balázs, G. Gy., Horváth, M., Schmidt, I., New Current Control Method for Grid-Connected Inverter of Domestic Power Plant, Proceedings of the 15th International Power Electronics and Motion Control Conference (EPE-PEMC 2012), pp.1-5. 2012

[23] Gyeviki J., Sárosi J., Csikós S., Position Control of Pneumatic Actuators with PLC, Proceedings of the IEEE/ASME International Conference on Advanced Intelligent Mechatronics (AIM2011), pp.742-747, 2011

[24] Mester, Gy., Matijevics, I., Szepe, T., Simon, J., Wireless Sensor-Based Robot Control, in: Application and Multidisciplinary Aspects of Wireless Sensor Networks Concepts, Integration, and Case Studies: Computer Communications and Networks, pp. 275-277, Springer, 2011

[25] Horváth, L., Rudas, I.J., New Method of Knowledge Representation and Communication for Product Object Modeling, Proceedings of the 12th WSEAS International Conference on Applied Computer Science ACS-12, pp. 75-80, 2012

[26] Bencsik, A.L., Gáti, J., Kártyás, Gy., Maintenance of Complex Automated Systems, 7th IEEE International Symposium on Applied Computational Intelligence and Informatics SACI-2012, pp. 223-227, 2012

[27] Dumitru, C., Gligor, A., Modeling and Simulation of Renewable Hybrid Power System Using Matlab/Simulink Environment, Scientific Bulletin of the „Petru Maior" University of Târgu Mureş, Vol.7, No.2, pp.5-9, 2010

[28] Nagy,I., Bencsik, A.L., A Global Path Planning Algorithm, Based on Maximal Localization Error, Proceeding of the Int. Jubilee Conf. Science in Engineering, Economics and Education, Budapest, Hungary, pp.69-85, 2005